Check for updates

Power scaling of ultrafast oscillators: 350-W average-power sub-picosecond thin-disk laser

F. SALTARELLI,[1,*] I. J. GRAUMANN,[1] L. LANG,[1] D. BAUER,[2] C. R. PHILLIPS,[1] AND U. KELLER[1]

[1]*Institute for Quantum Electronics, ETH Zurich, 8093 Zurich, Switzerland*
[2]*TRUMPF Laser GmbH, Aichhalder Straße 39, 78713 Schramberg, Germany*
[*]saltarelli@phys.ethz.ch

Abstract: We report a semiconductor saturable absorber mirror (SESAM)-modelocked thin-disk laser oscillator delivering a record 350-W average output power with 940-fs, 39-μJ pulses at 8.88-MHz repetition rate and 37-MW peak power. This oscillator is based on the Yb:YAG gain material and has a large pump spot on the disk. The cavity design includes an imaging scheme, which results in multiple reflections on the disk gain medium to enable a larger output coupling rate compared to those used in thin-disk oscillators with a single reflection on the disk. This reduces the intracavity power for a given output power, thus decreasing the stress on the intracavity components. We operate the laser in a low-pressure environment in order to limit the disk's thermal lensing and drastically reduce the nonlinearity picked up in the intracavity air medium. The combination of the imaging scheme and low-pressure operation paves the way to further power scaling of ultrafast thin-disk oscillators toward the kW milestone.

1. Introduction

Many industrial and scientific applications greatly benefit from ultrafast laser sources with megahertz repetition rate and multi-100-W average output power [1,2]. The current state of the art in terms of average power is achieved with diode-pumped laser amplifier systems based on fiber [3], slab [4], and thin-disk [5,6] technologies, each of which leverages a high surface-to-volume ratio for efficient heat removal. These systems can achieve more than 1 kW of average output power. By coherently combining multiple fiber amplifiers, up to 3.5 kW of average power have been demonstrated [3].

In this paper, we focus on the thin-disk laser (TDL) technology [7]. In TDLs, the gain medium is shaped as a disk, with a typical thickness of around 100 μm and is used in reflection inside the laser cavity. The pump and laser beams have a diameter of a few millimeters on the disk. The heat is extracted through the backside of the disk. This results in a quasi-1D heat flow which ensures optimal heat management and thus enables straightforward power scaling by increasing simultaneously the pump spot and the laser spot size on the disk. Amplifier systems based on the TDL technology achieved up to 2-kW average output power with 6.7-mJ pulses in a multi-pass configuration [5,6] and 1-kW average output power with 200-mJ 1.1-ps pulses in a regenerative amplifier configuration [8].

The reduced thickness and high-gain per unit length of the thin-disk gain medium make this technology ideal for the development of high-power ultrafast oscillators. In fact, the short interaction length between the pulses and the gain medium results in a sufficiently small amount of nonlinearity that modelocked pulse formation is not hindered. Hence, thin disks allow for the generation of high-power laser pulses directly from a high-power modelocked oscillator, bypassing the complexity of multi-stage ultrafast amplifier systems. Additionally, the timing jitter and limited repetition rate of regenerative amplifiers is avoided, as well as amplified spontaneous emission added by amplifier chains [9]. Moreover, TDLs offer by far the highest average power and pulse energy of any ultrafast oscillator technology [10]. They deliver a low-noise output

[11], megahertz repetition rates, and diffraction-limited beam quality from a single-box, diode-pumped laser source. These features enabled applications such as high-harmonic generation to the extreme ultraviolet [11] and optical rectification to the THz [12] directly from a laser oscillator. Additionally, the high intracavity power in TDL oscillators can be leveraged to drive intracavity nonlinear-optics experiments [13]. Finally, the recent demonstrations of multi-pass cell compression at 375-W average output power to 170 fs [14] and at 60 W to 16 fs pulses [15], show the possibility to compress the high-power output of these oscillators in order to get the optimal peak power for many nonlinear optics applications.

Over the last twenty years, the performance of modelocked TDLs has been continuously improved. We present in Fig. 1 an overview of how the average power was scaled over time focusing on Yb:YAG thin disks, which is the current leading gain material for high power. The first ultrafast TDL oscillator was demonstrated in the year 2000 using an Yb:YAG disk, and a semiconductor saturable absorber mirror (SESAM) for modelocking. It delivered 16-W average output power [16]. This result was later scaled to 80-W average output power due to improvements in the disk's quality and mitigation of the thermal effects [17]. These first ultrafast TDL oscillators were operated in air and based on short cavities encompassing a single reflection on the disk gain medium. Because of the limited gain from the disk, low output coupling rates of around 10% were used, resulting in very high intracavity average and peak powers. In fact, once few-μJ pulse energies and sub-ps pulse durations were achieved, the peak power became sufficient to induce strong self-phase modulation (SPM) from the nonlinear refractive index of the intracavity air [18]. This SPM (of order 1 rad or more) would need to be balanced with group delay dispersion (GDD) (of order 10^4–10^5 fs^2) for soliton pulse formation. The large negative GDD could be obtained through dispersive mirrors, which however have worse thermal behavior compared to standard dielectric mirrors and cause thermo-optic distortions at high intracavity powers [10]. In order to tackle the simultaneous challenges of having enough negative GDD and limiting the intracavity power, different approaches have been suggested in literature. One approach consists in designing a cavity encompassing multiple reflections on the disk gain medium in order to increase the round-trip gain, allowing the laser to be operated with a large output coupling rate. This approach led to the demonstration of a TDL oscillator with 11 reflections on the disk, delivering 145-W average output power with 41-μJ pulses [19]. Another approach consists in operating the laser in a low-pressure environment (few mbar of air) or in a Helium atmosphere in order to decrease the amount of SPM accumulated in the intracavity atmosphere and thereby reduce the required GDD by an order of magnitude or more [18]. This is the approach which led to the previous record: a 275-W average power SESAM-modelocked TDL oscillator with 17-μJ pulses demonstrated in 2012 [20]. Additionally, this approach led to the demonstration of the thin-disk oscillator delivering the highest pulse energy to date, that is 80 μJ at 242-W average output power [21].

Kerr-lens modelocking (KLM) has also been employed in order to modelock TDL oscillators. In its first demonstration in 2011, 45-W average output power was achieved [22], and shortly thereafter, a KLM TDL matched the performance of SESAM-modelocked TDLs with 270-W average output power at 14-μJ pulse energy [23]. Both results have been achieved in an air environment and delivered shorter pulses at higher repetition rate compared to the presented high-power SESAM-modelocked Yb:YAG thin-disk oscillators [19–21]. Recently, a KLM Yb:YAG thin-disk oscillator designed with an active multi-pass configuration and delivering 140-W average power at 13-μJ pulse energy has been demonstrated [24].

Power scaling of thin-disk lasers requires increasing the spot size on the disk in order to avoid damaging the gain material. For example, without laser operation we have observed damage when operating at 5.4-kW/cm^2 pump intensity and 8-mm-diameter pump spot on an Yb:YAG thin disk. In the discussed ultrafast TDL oscillators [16–24], the pump spot was at most 4.7-mm in diameter, which limits the pump power to ≈1 kW when keeping within a safe intensity regime.
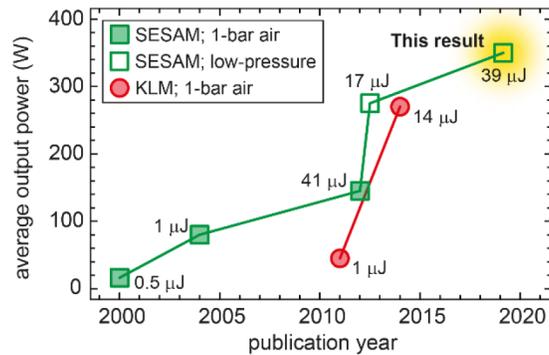
Fig. 1. Average output power from Yb:YAG SESAM-modelocked and KLM oscillators, which represented a new record at the time of publication. The labels indicate the output pulse energy. References are provided in the text. In this result we combine a cavity design including multiple reflections on the disk gain medium with operation in a low-pressure environment.

However, scaling the beam size on the disk and on other optical components comes at the cost of an increased sensitivity to the thermal lensing of those components [25]. This increased sensitivity renders it hard to operate thin-disk oscillators in fundamental-spatial mode with large pump spots and, combined with the pre-existing challenges, hindered further power scaling of these results until now.

Here we present a TDL oscillator (Fig. 2) with a large 6-mm-diameter pump spot on the disk. In order to overcome the mentioned challenges associated with the large pump spot and keep the intracavity power low to reduce the stress on the intracavity components, we combined an imaging scheme for multiple reflections on the disk with low-pressure operation. Additionally, we carefully arranged the mirrors in the cavity in order to keep the angle of incidence on the curved mirrors small and hence avoid astigmatism. We obtained 350-W average output power with 940-fs, 39-μJ pulses at 8.88-MHz repetition rate and 37-MW peak power. To the best of our knowledge, this is the highest average power obtained at the output of any modelocked laser
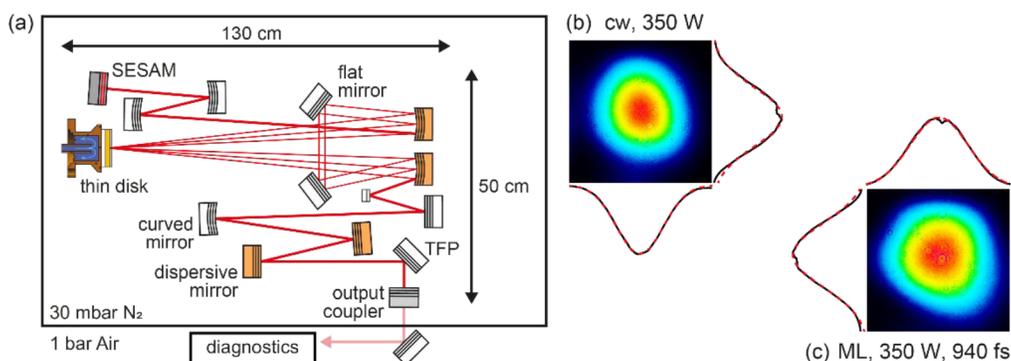

Fig. 2. (a) Schematic of the cavity design, including three reflections on the disk gain medium. TFP: thin-film polarizer; (b) beam profile at 350-W output power in cw operation, i.e., with the SESAM replaced by a HR mirror; (c) beam profile at 350 W in modelocked operation. The beam profiles are acquired by imaging the leakage of a mirror in a position ≈ 0.85 m from the SESAM. The horizontal and vertical cuts of the beam through the center of mass are presented together with gaussian fits (in red).

oscillator. Additionally, we demonstrate modelocked operation with a pump spot size compatible with pumping at 1.5 kW and hence more than 500-W average output power.

We detail the cavity design in Section 2 and analyze the performance of the laser in continuous-wave (cw) and modelocked operation in Section 3. We conclude in Section 4 by presenting an outlook on the scaling prospects of ultrafast thin-disk oscillators.

2. Cavity design

Power scaling thin-disk oscillators involves simultaneously increasing the pump and laser spot size on the disk. This approach has been extremely successful, in fact cw thin-disk oscillators delivering up to 10 kW in multi-mode operation have been demonstrated [26].

Modelocked operation imposes additional requirements: the cavity needs to be operated in fundamental transverse mode, must incorporate a saturable-loss device, and nonlinearity needs to be managed [10,27]. The larger laser spot on the disk leads, to a larger spot throughout the cavity and hence on the intracavity components. This makes the cavity more susceptible to static and thermo-optical wavefront distortions on many intracavity components such as the disk, the dispersive mirrors, and the SESAM, especially for cavities including multiple reflections on the disk. The width of the stability zone [Fig. 3(b)] with respect to disk's thermal lensing scales inversely with the square of the laser-spot size on the disk, for a fixed number of intracavity passes over the gain medium [25]. Thus, achieving fundamental mode operation over an extended power range becomes more challenging for increased laser-spot sizes.
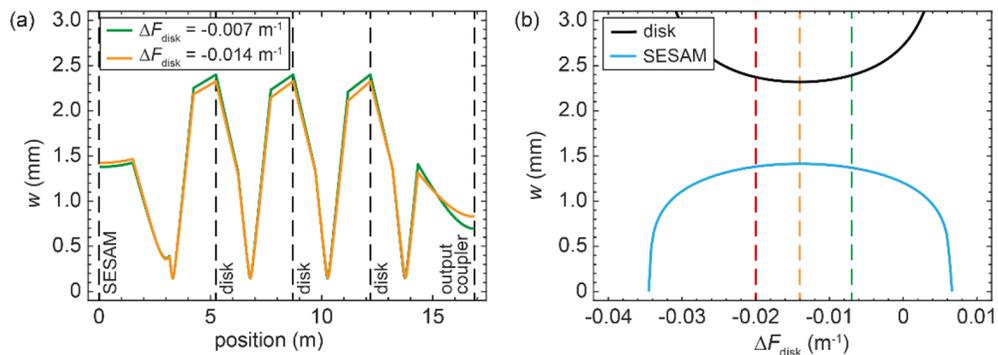

Fig. 3. (a) Evolution of the $1/e^2$ mode radius as a function of the position inside the laser cavity. $\Delta F_{\mathrm{disk}} = 0$ corresponds to the cold disk. The green line assumes the disk's focusing power at lasing threshold and the orange line at the middle of the stability zone; (b) stability zone: calculated beam radius at the position of the disk (black line) and the SESAM (light blue line) as a function of the disk's focusing power change ΔF_{disk}. The vertical green and orange dashed lines represent the disk's focusing power values used for Fig. 3(a); the red dashed line the focusing power at the maximum output power. We optimized the cavity such that going from low to high power, we move around the center of the stability zone.

To modelock high-power oscillators, the SESAM is particularly well suited since pulse formation is decoupled from cavity stability, hence disentangling fundamental spatial-mode operation and modelocking. Additionally, the thin structure of the SESAM compared to the beam size ensures an efficient heat extraction analogous to the gain disk and its parameters can be adjusted via semiconductor engineering. To obtain sub-ps pulses in SESAM-modelocked lasers despite the presence of a slow saturable loss, we rely on soliton pulse shaping effects [28]. This process is based on a balance between intracavity GDD typically obtained through Gires-Tournois interferometer (GTI)-type dispersive mirrors, and SPM. The dispersive mirrors, because of their resonant structure, have worse thermal behavior compared to high-reflective

dielectric mirrors based on distributed Bragg reflection (DBR) structures [10]. The SESAM also has some thermal lensing determined by its small non-saturable losses, which are typically of order 0.1% in state-of-the-art SESAMs [29]. Operating these components at kW-level intracavity average power results in thermo-optic distortions, which ultimately hinder pulse formation, limiting the achievable output power.

In order to mitigate these thermal effects, a compelling approach is to reduce the intracavity power by designing an imaging scheme in the laser cavity encompassing multiple reflections on the disk gain medium and, hence, allowing a larger output coupling rate [19,24,27]. However, such an imaging scheme further increases the sensitivity to the disk's thermal lensing. In fact, the width of the stability zone scales as the reciprocal of the number of passes on the disk. Hence this approach was avoided for the previous power-scaling result [20]. We recently developed a better understanding of the sources of thermal lensing in thin-disk lasers, and, particularly, discovered that a substantial contribution to the disk's thermal lensing originates in the heated air in front of the disk [30]. We removed this contribution by operating the laser in a low-pressure environment and optimized the laser cavity accounting for the change in thermal lens between air operation (during alignment) and low-pressure operation (during modelocking). In this way, we also drastically reduced the amount of SPM picked up in the intracavity air, hence reducing the amount of GDD needed for soliton pulse formation by an order of magnitude.

In our oscillator, we employed a 100-μm thick, 10-at.% doped Yb:YAG disk, contacted on a concave diamond with a cold radius of curvature $R_{cold} = 3.80$ m (TRUMPF GmbH). We pumped the disk with a 6.0-mm-diameter pump spot through a 44-pass thin-disk head using free-space-coupled diodes able to deliver up to 3 kW at 938 nm. We limited the pump power to 1.4 kW corresponding to 5.0 kW/cm^2 of pump intensity in order to avoid damaging the disk. At this power the diodes emit at 930 nm. We designed an imaging scheme with two 2-m concave dispersive mirrors encompassing three reflections on the disk to support a comparatively large $T_{OC} = 25\%$ transmission output coupler [Figs. 2(a) and 3(a)]. A larger output coupling rate (for example of 40% as in [27]) would have been possible, however we found that larger output coupling rates resulted in a reduced optical-to-optical efficiency and hence additional thermal load on the disk. Each bounce on the 2-m dispersive mirrors inside the active multi-pass cell results in -550 fs^2 of GDD. Hence, we obtain -6'600 fs^2 of round-trip GDD directly from the active multi-pass cell, i.e., 2-m concave mirrors, disk, and 45° high-reflective flat mirrors. On the SESAM arm of the cavity we implemented a telescope using a 300-mm concave mirror and a 3-m concave mirror in order to have the optimal spot size with respect to the saturation property of our SESAM. This results in a designed 1/e^2 laser spot radius on the SESAM $w_{SESAM} \approx 1.35$ mm.

Fundamental spatial-mode operation in thin-disk oscillators is achieved by optimizing the laser spot to pump spot ratio. Empirically, the optimal ratio is known to be $\approx 75\%$. This ensures that higher order modes, due to their larger transverse size, are disfavored and thus fundamental spatial mode operation is achieved. Thermal lensing on the disk results in a change of the disk's radius of curvature R, quantified by the change in focusing power: $\Delta F_{disk} = 2/R_{cold} - 2/R(T)$, where T is the temperature of the disk. We measured the ΔF_{disk} with an interferometer and the disk's temperature T with a thermal camera (FLIR) without laser operation. Hence, by measuring T during laser operation and taking into account the difference in focusing power between air and low-pressure operation, we can infer ΔF_{disk}, as described in [30]. We have $\Delta F_{disk} \approx$ -0.007 m^{-1} for laser operation just above threshold and $\Delta F_{disk} \approx$ -0.020 m^{-1} at 350-W output power in modelocked operation. We thus optimized the cavity design in order to have the center of the stability zone at -0.014 m^{-1}, in order to minimize the change in laser beam radius on the disk over an extended power range (Fig. 3).

In addition to the challenges due to thermal lensing, the finite angle of incidence on the curved mirrors leads to a difference in the effective curvature of these mirrors in the vertical and horizontal direction. This results in cavity astigmatism and a shift in the stability zone. This

effect is particularly relevant on the 2-m concave mirrors employed in the active multi-pass cell because of the large spot size on these mirrors [they are located before and after the disk, see Fig. 3(a)]. In order to avoid any significant astigmatism problems we employed two Newport Suprema Clear Edge 2" mirror mounts to place the 2-m concave mirrors almost in touch with each other and hence limit the angle of incidence on the disk to $< 2.5°$ and on these mirrors to $< 1.5°$. The angles of incidence on the other curved mirrors in the cavity was $< 2°$ by folding the cavity. By following these measures of precaution, the astigmatic effects are negligible and proper operation of the laser over the full range of output powers has become possible.

3. Laser performance in continuous wave and modelocked operation

For stable SESAM modelocking the cavity should operate in fundamental spatial mode. Hence, we first characterized the oscillator without the SESAM and with only the $-6'600$ fs^2 of round-trip GDD coming from the dispersive mirrors in the active multi-pass cell. In this configuration we obtained up to 570 W output power at 1.4 kW of pump power, corresponding to 41% optical-to-optical efficiency [red squares in Fig. 4(a)]. The beam quality stays diffraction limited over the whole range of power with an $M^2 < 1.05$.
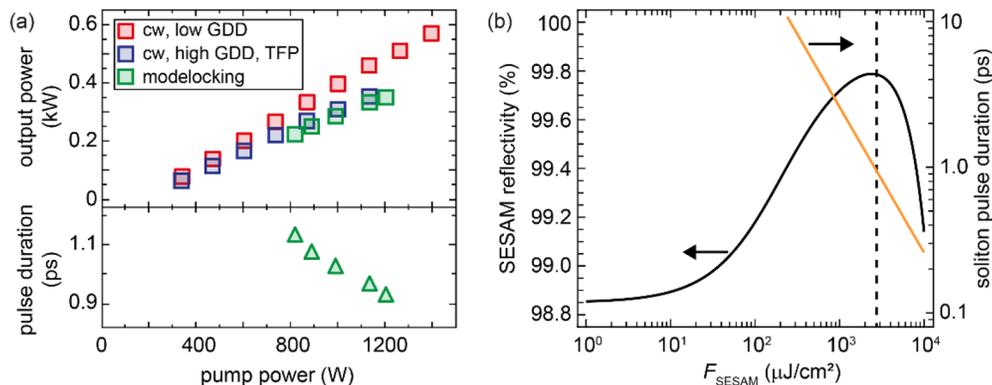

Fig. 4. Power slopes: (a) average output power and pulse duration versus pump power. Red squares refer to cw laser operation with -6'600 fs^2 of round-trip GDD. Blue and green squares refer to a laser configuration with -16'600 fs^2 of GDD and including a TFP, in cw and modelocked operation, respectively; (c) saturation properties of the SESAM: reflectivity for a Gaussian beam versus spatially-averaged fluence on the SESAM (black line). For this calculation we assume that the pulse duration scales inversely to the pulse energy (orange line), as in soliton pulse shaping. The operating point at 350-W average output power, 940-fs pulse duration is marked with a vertical dashed line.

The next step was to introduce the dispersion required for soliton pulse formation, we replaced four flat DBR mirrors with GTI-type dispersive mirrors, two of them introducing -500 fs^2 of GDD per bounce (Layertec GmbH) and two of them introducing -2'000 fs^2 of GDD per bounce (University of Neuchatel). In this way we have a total of -16'600 fs^2 of round-trip GDD from the mirrors. Additionally, we introduced a thin-film polarizer (TFP) in the laser cavity in order to fix the polarization of the laser. We again tested this cavity in cw operation obtaining fundamental mode operation ($M^2 < 1.10$) at up to 350 W output power with 1.1 kW of pump power, corresponding to 31% optical-to-optical efficiency [blue squares in Fig. 4(a) and beam profile in Fig. 2(b)]. There is a $\approx 10\%$ loss in optical-to-optical efficiency compared to the same laser cavity without the additional dispersive mirrors and the TFP. This is most likely due to the additional losses introduced by the TFP and the thermal effects in the dispersive mirrors which alter the cavity mode and introduce non-spherical aberrations. Additionally, the lower

optical-to-optical efficiency translates into a larger thermal load on the disk due to the reduced heat extraction through lasing and hence additional thermal lensing.

Lastly, we replaced the end mirror with a SESAM designed for high-power operation [31]. The SESAM was grown and contacted to a copper mount in the ETH Zurich FIRST cleanroom facility. It consists of a DBR and three InGaAs quantum wells as absorber in an anti-resonant configuration. It has a saturation fluence of 120 μJ/cm^2, a modulation depth of 1.1%, non-saturable losses of $\approx 0.1\%$, and a two-photon absorption (TPA) coefficient $F_2 = 650$ mJ/cm^2 for 130-fs pulses [32].

We operated the laser in a 30-mbar N_2 atmosphere resulting in a SPM coefficient of ≈ 0.3 mrad/MW per cavity roundtrip, defined as the ratio between the B-integral and the intracavity peak power. Additionally, we estimate a contribution of ≈ 0.3 mrad/MW of SPM from the coatings of the dispersive mirrors based on the measured pulse duration and assuming soliton pulse formation [27,33]. The SPM accumulated in the thin-disk and in the SESAM is negligible. The laser shows stable modelocking from 220-W output power with 1.14-ps pulses up to 350-W output power with 940-fs pulses at 1.2 kW of pump power [green symbols in Fig. 4(a) and beam profile in Fig. 2(c)] (power meter: Coherent PM LM-5000). This corresponds to an optical-to-optical efficiency of 29%. We note that this is only 2% lower compared to the efficiency in cw operation in the same laser configuration, confirming the very low non-saturable losses of the employed SESAM.

We monitored the beam profile of the laser imaging the leakage of a mirror in a position ≈ 0.85 m from the SESAM. The expected 1/e^2 beam radius from ABCD matrix calculation, at that position in the cavity, is ≈ 1.4 mm [Fig. 3(a)]. For comparison, we took cuts along the horizontal and vertical axes of the measured beam profiles in cw and modelocked operation. The cuts are shown in Figs. 2(b) and 2(c) together with Gaussian fits, showing close agreement. Regarding the 1/e^2 mode radius, we find in cw a slightly astigmatic beam with an average beam radius of 1.35 mm and in modelocked operation a symmetric beam with an average mode radius of 1.6 mm. These values are within 15% of the expected beam size. The slightly larger beam radius in modelocked operation may be due to the different thermal load on the disk because of the slightly lower optical-to-optical efficiency and the thermal lensing of the SESAM. The modelocking dynamics of femtosecond solid-state lasers with a slow saturable absorber is often approximated by soliton pulse shaping [28]. A signature of this modelocking regime is that the pulse duration decreases with increasing pulse energy, which we also find in our oscillator [Fig. 4(a)]. In the soliton-modelocking regime the saturable absorber starts and stabilizes the modelocking process while the pulses are shaped by the balance between GDD and SPM. This results in *sech*^{2}-shaped pulses. Hence, we fitted the laser diagnostics assuming this pulse shape and extracted the spectrum full-width-half-maximum (FWHM) and the pulse duration from the fits. At 220-W average output power, we have 1.14-ps pulses and a spectrum FWHM of 1.27 nm (time-bandwidth product, TBP $= 1.30 \times 0.315$), at the maximum output power of 350 W (Fig. 5) we have 940-fs pulses and a spectrum FWHM of 1.63 nm (TBP $= 1.36 \times 0.315$). We notice that the pulses are longer than the transform-limited duration, suggesting that they could be chirped. Further investigation will be necessary in order to understand the causes. The diagnostics in Fig. 5 at the maximum output power (350 W) shows stable modelocking. We acquired large span microwave spectrum analyzer (Hewlett Packard 8562E) traces and, additionally, scanned a long-range (200 ps) autocorrelator (Femtochrome FR-103XL) to confirm single-pulse operation. In this experiment, we decided to not increase the power further to prevent the disk from overheating in case laser operation was interrupted due to misalignment or SESAM damage. A planned safety interlock to switch off the pump in case of non-lasing conditions will allow safe operation at even higher powers in the future.

Furthermore, we calculated the nonlinear reflectivity curve of the employed SESAM, taking into account soliton pulse shaping [34] [Fig. 4(b)]. The TPA coefficient F_2, characterizing the strength of the inverse saturable absorption, scales linearly with the pulse duration. We
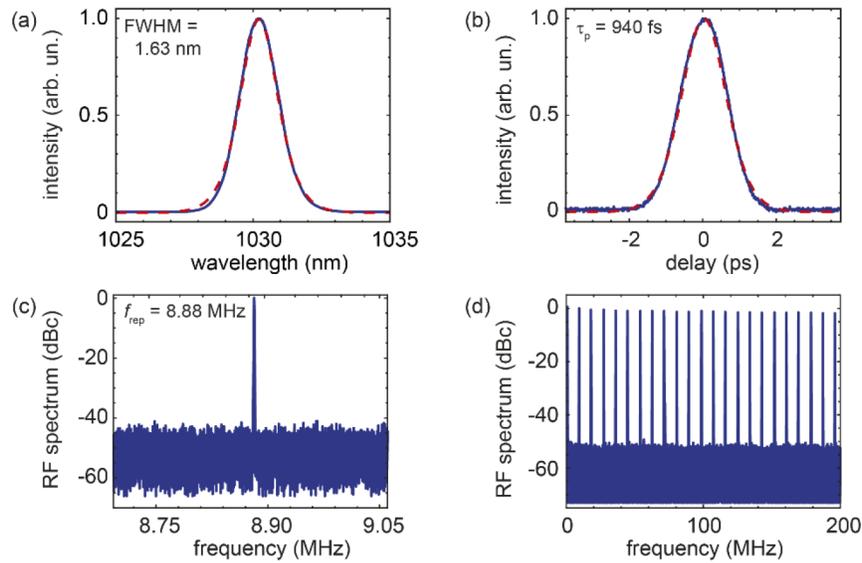
Fig. 5. Laser diagnostics at 350-W output power. (a) Optical spectrum; (b) intensity autocorrelator; microwave spectrum (c) centered on the peak at the repetition rate with 300 Hz resolution bandwidth and noise floor around −42 dBc and (d) showing the harmonics with 10 kHz resolution bandwidth and noise floor around −50 dBc. Red dashed lines in (a) and (b) are fits assuming *sech*^{2}-shaped pulses, the resulting FWHM of the optical spectrum and the pulse duration from the fits are reported in the corresponding figures.

therefore take our experimental modelocking point at 39 μJ, 940 fs as a reference and calculate the expected pulse duration τ_p at any given pulse energy E_p according to soliton pulse shaping $\tau_\text{p} \sim 1/E_\text{p}$. The spatially-averaged incident fluence on the SESAM is calculated according to $F_\text{SESAM} = E_p/(\pi\, T_{OC}\, w_\text{SESAM}^2)$ [32]. At the maximum output power in modelocked operation we have $F_\text{SESAM} = 2.7$ mJ/cm^2 [Fig. 4(b), vertical dashed line]. This lies close to the maximum of the SESAM reflectivity curve. Operation slightly further into the rollover is possible but at the expenses of additional losses and hence thermal load on the SESAM [34].

4. Conclusion and outlook

In conclusion, we demonstrated an ultrafast laser oscillator based on the thin-disk technology delivering 350-W average output power with 940-fs pulses at 8.88-MHz repetition rate. This represents, to the best of our knowledge, the highest average power achieved from any modelocked ultrafast oscillator. We obtained this record result by using a thin-disk head with a large pump spot on the disk and tackling the resulting cavity stability challenges through an imaging scheme encompassing multiple reflections on the disk gain medium and low-pressure operation.

A roadmap for further power scaling of this laser architecture beyond 500-W output power consists in designing an active multi-pass cell encompassing five rather than three reflections on the disk and hence increasing the output coupling rate to 40% from the current 25%. Thin-disk oscillators based on the Yb:YAG gain material and operating with even larger output-coupling rates have already been demonstrated [19,24,27]. For this purpose, 2"-diameter mirrors inside the multi-pass cell can be used to accommodate the multiple reflections. The same intracavity power we use here would then yield 550 W output power, while keeping the spot size on the SESAM similar to the current configuration and thus avoiding additional thermal effects or aberrations from this component. A further step in power scaling toward the kW level could be done by

actively compensating the thermal lensing of the intracavity components via a deformable mirror, which has already been demonstrated in cw at kW-level output power [35] and the development of large-area SESAMs with improved thermal characteristics [29].

This result shows the possibility to develop sources combining multi-100-W average output power with the simplicity and high repetition rates of oscillators. Additionally, its output pulse energy of 39 µJ makes it a compelling source for high-field physics experiments such as high-repetition-rate high-harmonic generation and for industrial applications such as laser micromachining.

Disclosures

The authors declare no conflicts of interest.

References

1. S. Nolte, F. Schrempel, and F. Dausinger, "Ultrashort Pulse Laser Technology," in *Springer Series in Optical Sciences*, (Springer International Publishing, 2016).
2. T. Südmeyer, S. V. Marchese, S. Hashimoto, C. R. E. Baer, G. Gingras, B. Witzel, and U. Keller, "Femtosecond laser oscillators for high-field science," Nat. Photonics **2**(10), 599–604 (2008).
3. M. Müller, A. Klenke, A. Steinkopff, H. Stark, A. Tünnermann, and J. Limpert, "3.5 kW coherently combined ultrafast fiber laser," Opt. Lett. **43**(24), 6037–6040 (2018).
4. P. Russbueldt, T. Mans, J. Weitenberg, H. D. Hoffmann, and R. Poprawe, "Compact diode-pumped 1.1 kW Yb:YAG Innoslab femtosecond amplifier," Opt. Lett. **35**(24), 4169–4171 (2010).
5. J.-P. Negel, A. Loescher, A. Voss, D. Bauer, D. Sutter, A. Killi, M. A. Ahmed, and T. Graf, "Ultrafast thin-disk multipass laser amplifier delivering 1.4 kW (4.7 mJ, 1030 nm) average power converted to 820 W at 515 nm and 234 W at 343 nm," Opt. Express **23**(16), 21064–21077 (2015).
6. J.-P. Negel, A. Loescher, D. Bauer, D. Sutter, A. Killi, M. A. Ahmed, and T. Graf, "Second Generation Thin-Disk Multipass Amplifier Delivering Picosecond Pulses with 2 kW of Average Output Power," in *Lasers Congress 2016 (ASSL, LSC, LAC)*, OSA Technical Digest (online) (Optical Society of America, 2016), ATu4A.5.
7. A. Giesen, H. Hugel, A. Voss, K. Wittig, U. Brauch, and H. Opower, "Scalable Concept for Diode-Pumped High-Power Solid-State Lasers," Appl. Phys. B: Lasers Opt. **58**(5), 365–372 (1994).
8. T. Nubbemeyer, M. Kaumanns, M. Ueffing, M. Gorjan, A. Alismail, H. Fattahi, J. Brons, O. Pronin, H. G. Barros, Z. Major, T. Metzger, D. Sutter, and F. Krausz, "1 kW, 200 mJ picosecond thin-disk laser system," Opt. Lett. **42**(7), 1381–1384 (2017).
9. C. M. Caves, "Quantum limits on noise in linear amplifiers," Phys. Rev. D **26**(8), 1817–1839 (1982).
10. C. J. Saraceno, F. Emaury, C. Schriber, A. Diebold, M. Hoffmann, M. Golling, T. Südmeyer, and U. Keller, "Toward millijoule-level high-power ultrafast thin-disk oscillators," IEEE J. Sel. Top. Quantum Electron. **21**(1), 106–123 (2015).
11. F. Emaury, A. Diebold, C. J. Saraceno, and U. Keller, "Compact extreme ultraviolet source at megahertz pulse repetition rate with a low-noise ultrafast thin-disk laser oscillator," Optica **2**(11), 980–984 (2015).
12. F. Meyer, N. Hekmat, S. Mansourzadeh, F. Fobbe, F. Aslani, M. Hoffmann, and C. J. Saraceno, "Optical rectification of a 100 W average power mode-locked thin-disk oscillator," Opt. Lett. **43**(24), 5909–5912 (2018).
13. F. Labaye, M. Gaponenko, V. J. Wittwer, A. Diebold, C. Paradis, N. Modsching, L. Merceron, F. Emaury, I. J. Graumann, C. R. Phillips, C. J. Saraceno, C. Kränkel, U. Keller, and T. Südmeyer, "Extreme ultraviolet light source at a megahertz repetition rate based on high-harmonic generation inside a mode-locked thin-disk laser oscillator," Opt. Lett. **42**(24), 5170–5173 (2017).
14. J. Schulte, T. Sartorius, J. Weitenberg, A. Vernaleken, and P. Russbueldt, "Nonlinear pulse compression in a multi-pass cell," Opt. Lett. **41**(19), 4511–4514 (2016).

15. K. Fritsch, M. Poetzlberger, V. Pervak, J. Brons, and O. Pronin, "All-solid-state multipass spectral broadening to sub-20 fs," Opt. Lett. **43**(19), 4643–4646 (2018).

16. J. Aus der Au, G. J. Spühler, T. Südmeyer, R. Paschotta, R. Hövel, M. Moser, S. Erhard, M. Karszewski, A. Giesen, and U. Keller, "16.2 W average power from a diode-pumped femtosecond Yb:YAG thin disk laser," Opt. Lett. **25**(11), 859–861 (2000).

17. F. Brunner, E. Innerhofer, S. V. Marchese, T. Südmeyer, R. Paschotta, T. Usami, H. Ito, S. Kurimura, K. Kitamura, G. Arisholm, and U. Keller, "Powerful red-green-blue laser source pumped with a mode-locked thin disk laser," Opt. Lett. **29**(16), 1921–1923 (2004).

18. S. V. Marchese, T. Südmeyer, M. Golling, R. Grange, and U. Keller, "Pulse energy scaling to 5 μJ from a femtosecond thin disk laser," Opt. Lett. **31**(18), 2728–2730 (2006).

19. D. Bauer, I. Zawischa, D. H. Sutter, A. Killi, and T. Dekorsy, "Mode-locked Yb:YAG thin-disk oscillator with 41 μJ pulse energy at 145 W average infrared power and high power frequency conversion," Opt. Express **20**(9), 9698–9704 (2012).

20. C. J. Saraceno, F. Emaury, O. H. Heckl, C. R. E. Baer, M. Hoffmann, C. Schriber, M. Golling, T. Südmeyer, and U. Keller, "275 W average output power from a femtosecond thin disk oscillator operated in a vacuum environment," Opt. Express **20**(21), 23535–23541 (2012).

21. C. J. Saraceno, F. Emaury, C. Schriber, M. Hoffmann, M. Golling, T. Südmeyer, and U. Keller, "Ultrafast thin-disk laser with 80 μJ pulse energy and 242 W of average power," Opt. Lett. **39**(1), 9–12 (2014).

22. O. Pronin, J. Brons, C. Grasse, V. Pervak, G. Boehm, M. C. Amann, V. L. Kalashnikov, A. Apolonski, and F. Krausz, "High-power 200 fs Kerr-lens mode-locked Yb:YAG thin-disk oscillator," Opt. Lett. **36**(24), 4746–4748 (2011).

23. J. Brons, V. Pervak, E. Fedulova, D. Bauer, D. Sutter, V. Kalashnikov, A. Apolonskiy, O. Pronin, and F. Krausz, "Energy scaling of Kerr-lens mode-locked thin-disk oscillators," Opt. Lett. **39**(22), 6442–6445 (2014).

24. M. Poetzlberger, J. Zhang, S. Gröbmeyer, D. Bauer, D. Sutter, J. Brons, and O. Pronin, "Kerr-lens mode-locked thin-disk oscillator with 50% output coupling rate," Opt. Lett. **44**(17), 4227–4230 (2019).

25. V. Magni, "Multielement stable resonators containing a variable lens," J. Opt. Soc. Am. A **4**(10), 1962–1969 (1987).

26. S.-S. Schad, T. Gottwald, V. Kuhn, M. Ackermann, D. Bauer, M. Scharun, and A. Killi, "Recent development of disk lasers at TRUMPF," Proc. SPIE **9726**, 972615 (2016)..

27. F. Saltarelli, A. Diebold, I. J. Graumann, C. R. Phillips, and U. Keller, "Self-phase modulation cancellation in a high-power ultrafast thin-disk laser oscillator," Optica **5**(12), 1603–1606 (2018).

28. F. X. Kartner, I. D. Jung, and U. Keller, "Soliton mode-locking with saturable absorbers," IEEE J. Sel. Top. Quantum Electron. **2**(3), 540–556 (1996).

29. A. Diebold, T. Zengerle, C. G. E. Alfieri, C. Schriber, F. Emaury, M. Mangold, M. Hoffmann, C. J. Saraceno, M. Golling, D. Follman, G. D. Cole, M. Aspelmeyer, T. Südmeyer, and U. Keller, "Optimized SESAMs for kilowatt-level ultrafast lasers " Opt," Opt. Express **24**(10), 10512–10526 (2016).

30. A. Diebold, F. Saltarelli, I. J. Graumann, C. J. Saraceno, C. R. Phillips, and U. Keller, "Gas-lens effect in kW-class thin-disk lasers," Opt. Express **26**(10), 12648–12659 (2018).

31. C. J. Saraceno, C. Schriber, M. Mangold, M. Hoffmann, O. H. Heckl, C. R. E. Baer, M. Golling, T. Südmeyer, and U. Keller, "SESAMs for high-power oscillators: design guidelines and damage thresholds," IEEE J. Sel. Top. Quantum Electron. **18**(1), 29–41 (2012).

32. D. J. H. C. Maas, B. Rudin, A.-R. Bellancourt, D. Iwaniuk, S. V. Marchese, T. Südmeyer, and U. Keller, "High precision optical characterization of semiconductor saturable absorber mirrors," Opt. Express **16**(10), 7571–7579 (2008).

33. J. Herrmann, "Theory of Kerr-lens mode locking: role of self-focusing and radially varying gain," J. Opt. Soc. Am. B **11**(3), 498–512 (1994).

34. I. J. Graumann, A. Diebold, C. G. E. Alfieri, F. Emaury, B. Deppe, M. Golling, D. Bauer, D. Sutter, C. Kränkel, C. J. Saraceno, C. R. Phillips, and U. Keller, "Peak-power scaling of femtosecond Yb:Lu$_2$O$_3$ thin-disk lasers," Opt. Express **25**(19), 22519–22536 (2017).

35. S. Piehler, T. Dietrich, P. Wittmüss, O. Sawodny, M. A. Ahmed, and T. Graf, "Deformable mirrors for intra-cavity use in high-power thin-disk lasers," Opt. Express **25**(4), 4254–4267 (2017).